

Multi -Target Detection Capability of Linear Fusion Approach under Different Swerling Models of Target Fluctuation

Mohamed Bakry El_Mashade

Received: 6 June 2021 Accepted: 30 June 2021 Published: 15 July 2021

Abstract

In evolving radar systems, detection is regarded as a fundamental stage in their receiving end. Consequently, detection performance enhancement of a CFAR variant represents the basic requirement of these systems, since the CFAR strategy plays a key role in automatic detection process. Most existing CFAR variants need to estimate the background level before constructing the detection threshold. In a multi-target state, the existence of spurious targets could cause inaccurate estimation of background level. The occurrence of this effect will result in severely degrading the performance of the CFAR algorithm. Lots of research in the CFAR design have been achieved. However, the gap in the previous works is that there is no CFAR technique that can operate in all or most environmental varieties. To overcome this challenge, the linear fusion (LF) architecture, which can operate with the most environmental and target situations, has been presented.

Index terms— adaptive detection, non-coherent integration, fluctuating targets, swerling models, target multiplicity environments.

1 I. Introduction

adar systems are widely used for safety purposes. For case in point, they are utilized at airports to safely regulate the air traffic and in a military context, they are employed to defend against hostile missiles. The mission of the radar is to detect targets of interest and to discard those that don't concern a particular application.

Depending on the type of radar application, the system might be concerned with estimating the target radar cross section (RCS), measuring and tracking its position or velocity, imaging it, or providing fire control data to direct weapons to the target. In all of these practical applications, one of the most fundamental tasks of a radar is the detection; the process of examining the radar data and determining if it represents interference only, or interference plus echoes from a target of interest (ToI) [1][2][3][4][5].

The detection capability is one of the most significant factors in the behavior of such type of vital systems. Normally, the purpose of detection is to distinguish genuine target reflections from noise and clutter. More specifically, target detection can be regarded as a style of classification, which distinguishes whether the tested signal contains an echo from a target or just corresponds to the noise. This process relies on the thresholding criteria. This criteria has two philosophies: fixed and adaptive. Although the fixed threshold is simple in design, it has a misdetection and this procedure deprives the system from its ability to control the false alarm rate. This strategy of detection is useful for non-fluctuating targets of identical reflection models but fails when a mixture of different targets exists in radar's field of view (FoV). Therefore, variable threshold will be needed to cover such scenarios. For this reason, adaptive detection thresholds have been the subject of research for a long time. In other words, there is a demand for a detection process that is based on dynamic, instead of static, threshold to cope with those situations of inhomogeneous or changing clutter environment all over the search space. This is the objective of the second philosophy. Constant false alarm rate (CFAR) technology is the most popular target detection framework to address the issues associated with fixed threshold. This technology is crucial as a desired property for automatic target detection in an unknown and non-stationary background. In other words, CFAR is a property that is assigned to the processor in which the threshold, or gain control devices, guarantees

an approximately constant rate of false target detection when the noise/clutter level temporally varies. The feature of CFAR activates the threshold in such a way that it becomes adaptive to the local clutter environment. Thus, the CFAR mechanism maintains the amount of false alarm under supervision in a diverse background of interference. It should be taken into account that this approach doesn't come at no cost.

In radar applications which necessitate precision strikes for reduced risk and cost efficient operation with minimum possible guarantee damage, besides radar size, computation cost is major issue. The increased performance of the detection algorithm demands an increase in computation speed and device memory for every scan. Therefore, a trade-off between performance and cost has to be made [6][7][8][9][10].

A robust detector should not only find targets but also eliminate false alarms. Therefore, the general objective of all radar detection schemes is to ensure that false alarms don't fluctuate randomly. During the detection process, each cell is evaluated for the presence/absence of a target using a threshold. It is beneficial to be able to detect both high-and low-fidelity targets while maintaining constant false alarm rate. This is actually the function of the adaptive thresholding algorithm which most modern radar systems apply it in their detection process. Although there exists a large number of versions of CFAR circuits, cell-averaging (CA), order-statistics (OS), and trimmed-mean (TM) scenarios remain the most popular and well-understood techniques. In many cases, a single CFAR processor can hardly meet the complex radar operation environment. Thus, the concept of composite CFAR designing was introduced, to account for both homogeneous and heterogeneous situations. Based on this concept, fusion of particular decisions of the single CFAR detectors by appropriate fusion rules provides a better final detection. In this regard, the linear fusion (LF) approach is based on the parallel operation of the CA, OS, and TM types of CFAR techniques. However, the computational complexity may prevent the use of these more robust algorithms in favor of simple thresholding techniques, especially in automotive applications. Nevertheless, with the increasing prospect of reduction in hardware cost and availability of high-speed processors, the drift to high-performance algorithms is inevitable [11][12][13][14][15].

The behavior of the target detection processor can be significantly enhanced with the availability of the statistical characteristics of a target's radar crosssection (RCS). To achieve such interesting objective, Swerling proposed five models (SWI-SWV), to describe the RCS statistical properties, for practical objects, based on χ^2 -distribution with varying degrees of freedom. In SWI model, the target reflections in a single scan have a constant RCS magnitude (perfectly correlated), but it varies from scan-to-scan obeying χ^2 probability density function (PDF) with two-degrees of freedom. For SWII model, the PDF of RCS is the same as in SWI with the exception that it is independent from pulse-to-pulse instead of scan-to-scan. Because some objects have a dominant scatterer, SWIII mod uses a fourth-degree χ^2 -statistics to model the returned pulses. This model has the same characteristics as SWI style which has constant magnitude from pulse-to-pulse, but different from scan-to-scan. The RCS, in SWIII template, has the same description as SWI form with the difference that its PDF follows χ^2 -statistics with fourdegrees of freedom. The RCS, in SWIV pattern, varies from pulse-to-pulse, instead of scan-to-scan, with the same PDF of SWIII model. Finally, SWV mode is characterized by constant and perfectly correlated, from pulse-to-pulse and from scan-to-scan, echo pulses which corresponds to infinite degrees of freedom [10,13].

Our goal in this paper is to analyze LF-CFAR structure when this strategy uses non-coherent integration of M pulses to carry out its decision. The primary and the secondary outlying targets are assumed to be fluctuating in terms of four Swerling models (SWI-SWIV). Closed-form expression is derived for its performance in the absence as well as in the presence of interferers. A comparison of the tested scheme with its basic variants along with Neyman-Pearson (N-P) detector is also portrayed. The paper proceeds as follows. Section II formulates the problem of interest. The detection performance of the tested methodology along with its fundamental variants is analyzed in section III. Section IV portrays our numerical results to evaluate the accuracy of the theoretical derivation and substantiate the effectiveness of the proposed schemes. Finally, our useful conclusions are drawn in section V.

2 II. Statistical Background and Model Description

The basic demands of the limited warfare of the present era necessitate precision strikes of reduced risk and cost efficient operation with minimum possible guarantee damage. In order to reply such exact challenges, the capability of automatic detection is increasingly becoming more important to the defense community. Automatic detection can be achieved by setting a fixed threshold based on the interference power level. This construction operates with predictable performance if the interference belongs only to thermal noise. However, the ideality of operating environment of radar systems is scarcely verified. Therefore, technology of adaptation is of primary concern in the design of their future scenarios [15][16].

The ability of a weak echo detection by the radar receiver is limited by the noise energy that occupies the same spectrum as the signal. From this point of view, the process of detection is based on establishing a threshold level at the output of the receiver. This threshold must be adjusted in such a way that weak signals are detected, but not so low that allows noise peaks to cross it and give a false target. Thus, the proper threshold selection is dependent upon how important it is if a mistake is occurred because of failing to recognize a signal (miss probability) or falsely indicating the presence of a signal (false alarm probability). On the other hand, to cope with a changing clutter environment, there is a persistent need of dynamic and adaptive threshold. This threshold must be varied, up and down, in accordance with the background level for the false alarm rate to be maintained

at its pre-set value. A detector with this characteristic is designated as constant CFAR. Thus, the CFAR strategy is the main goal of the radar system designer.

For the CFAR circuit to be efficient, it must realize some characteristics. The more motivating features include rigorous fitting of the detection threshold to the clutter background, masking avoidance of closely spaced targets, low CFAR loss, and constructing a threshold that gives point as well as extended targets the chance to pass. Whatever the structure of the CFAR model is, the framework of sliding window is regarded as its basic arrangement. As Fig. (1) depicts, this window moves throughout the coverage area, and contains a set of reference cells (RC's) around the central cell, which is termed as cell under test (CUT). To alleviate self-interference in a real target echo, some guard cells (GCs) embrace CUT. These cells are used as buffer between CUT and the training cells. They are excluded from the background computation to insure that the CUT doesn't affect the threshold calculation. The declaration of the presence of a target is carried out if the power of CUT is greater than the power of both GCs and the estimated level. Each resolution cell has the chance to occupy the position of CUT. In this regard, the RC's that have been already processed constitute the leading subset, whilst those that have not yet occupied the center organize the lagging subset. The size selection of the sliding window is dependent upon rugged knowledge of the typical clutter background. Generally, the window length N should be as large as possible for the estimation process to be of good modality. Meanwhile, N is preferred to be compatible with the typical range extension of homogeneous clutter zones for the demand of identically distributed random variables to be statistically satisfied. Normally, the typical value of N lies in the 16-32 range.

The detection threshold is established as the product of the estimated noise power Z by a scaling factor T , which is imposed to verify the desired rate of false alarm, as Fig. (1) portrays. By comparing the content of CUT with the resulting threshold, the procedure will recommend that the signal is belonging to a target, if the magnitude of the CUT surpasses the calculated threshold. Otherwise, the signal is coming from interference and no target is present.

Most modern radar systems are of coherent type. This means that they receive the returned signal in a polar (amplitude and phase) form. In the radar receiver, the synchronous detector generates an inphase (I) and a quadrature (Q) components from the received signal. Whilst the in-phase component denotes the real part, the quadrature component represents the imaginary part of the received signal. Under the null hypothesis (H_0), the received noise for both I and Q channels is modeled as an independent and identically distributed (IID) Gaussian random process with zero mean and of variance $\sigma^2/2$. In addition, I and Q channels are statistically independent. Thus, the received noise is a complex Gaussian signal ($n = n_I + jn_Q$) with $\sigma = 0$ and $\sigma^2 = 2\sigma_n^2$.

After pulse compression, the signal passes through a rectifier, which converts the complex signal into an amplitude and phase. In this vein, there are two familiar types of rectifiers: linear and square-law detectors. The linear detector measures only the magnitude ($\sqrt{I^2 + Q^2}$) of the complex received signal, which follows the Rayleigh distribution. The square-law detector, on the other hand, measures only the power ($I^2 + Q^2$) of the linear detector, the distribution of which is exponential. For both types, the phase is uniformly distributed in the interval $[0, 2\pi]$ [17].

3 a) Neymann -Pearson Detector

The Neyman-Pearson (N-P) processor operates with a detection threshold which is imposed in such a way that for a desired rate of false alarm, the level of detection will be maximized. This threshold is fixed and is derived from a known interference PDF. Practically, the using of N-P detector necessitates: 1) the background interference is IID over all resolution cells, to which the fixed threshold is to be applied, 2) the interference is of statistical distribution the parameters of which are known, 3) the interference environment is homogenous.

Generally, the detection process is achieved at the output of the rectifier and yields one of three possible outcomes: correct decision, missed detection, or false alarm. A correct decision is one in which the detector correctly declares the presence/absence of a target. A missed detection is one in which the detector declares the absence of a target when in truth the measurement contains a target return. A false alarm occurs when the detector declares the presence of a target and in reality a target's return is not present in the measured data. Whilst the first outcome is specified by P_d , the second one represents its complement ($1 - P_d$). Therefore, P_d plays an important role in determining the first two outcomes. The last outcome is characterized by P_{fa} . Thus, once P_d and P_{fa} are calculated, the processor performance is completely evaluated.

Here, we are concerned with square-law type of signal rectifiers. Thus, as we have noted above, the squarelaw detected output for any range cell (z) has an exponential distribution, the general formulation of which is: (U_p) $f(z) = \frac{1}{\sigma^2} \exp(-z/\sigma^2)$

In the above expression, $U(\cdot)$ stands for the unit-step function. The value of σ^2 depends on the situation of operation and can take one of the following values: In the preceding formula, " γ " denotes the signal-to-noise ratio (SNR) of the ToI return, whereas " γ_0 " symbolizes the interference-to-noise ratio (INR) of the interfering target return, and " σ^2 " represents the background noise power.

Since the target returns and interference are of the stochastic nature, the performance of a signal's detector is characterized in terms of probabilities. For N-P procedure, these probabilities take the form [9]: $P_d = \int_{\tau}^{\infty} f(z) dz = 1 - \exp(-\tau/\sigma^2)$ if $\tau = \sigma^2 \ln(1/P_{fa})$

It may be rarely that a decision is made on the basis of a single transmitted pulse. More often, a lot of pulses are transmitted, and the resulting received signal is integrated or processed in some way to enhance, relative to

4 B) CONSTANT FALSE ALARM RATE (CFAR) DETECTOR

169 the mono-pulse case, the SNR. In this regard, to detect the target signal with some reasonable probability and
 170 to reject noise, the signal must be more strengthened than the noise. For M-pulses, the range cell (γ) has a
 171 PDF given by [1]: $f(\gamma) = \frac{1}{\Gamma(M)} \gamma^{M-1} \exp(-\gamma) = \exp(-\gamma) \gamma^{M-1} / \Gamma(M)$ (4)

172 The cumulative distribution function (CDF) corresponding to the PDF of Eq. (4) has a form given by: $F(\gamma) = 1 - \exp(-\gamma) \sum_{k=0}^{M-1} \frac{\gamma^k}{k!}$ (5)

173 In radar systems, detection performance is always related to target models and background environments.
 174 Thus, the availability of the statistical characteristics of a target's radar cross-section (RCS) can significantly
 175 ameliorate the performance of the detection algorithm. For this purpose, Swerling introduced five models (SWI-
 176 SWV), to describe the RCS statistical properties of the objects based on χ^2 distributions of varying degrees
 177 of freedom. For ν th degree of freedom χ^2 fluctuating target, the PDF of the target return is given by [9]: $f(\gamma) = \frac{1}{\Gamma(\nu/2)} \gamma^{\nu/2-1} \exp(-\gamma)$ (6)

178 $\Gamma(\nu/2)$ stands for the confluent hyper-geometric function and $\bar{\gamma}$ denotes the average M-pulse SNR. The
 179 calculation of the CDF associated with this PDF yields: $F(\gamma) = 1 - \exp(-\gamma) \sum_{k=0}^{\nu/2-1} \frac{\gamma^k}{k!}$ (7) with $\nu=2$ for SWI for M
 180 SWII for SWII for M SWI for $\nu=2$ (8)

181 $\Gamma(\nu/2)$ stands for the confluent hyper-geometric function and $\bar{\gamma}$ denotes the average M-pulse SNR. The
 182 calculation of the CDF associated with this PDF yields: $F(\gamma) = 1 - \exp(-\gamma) \sum_{k=0}^{\nu/2-1} \frac{\gamma^k}{k!}$ (7) with $\nu=2$ for SWI for M
 183 SWII for SWII for M SWI for $\nu=2$ (8)

184 The substitution of Eq. (7) into Eq. (8) and using the values indicated in Eq. (8), the N-P performance can
 185 be easily obtained for fluctuating targets of different Swerling's models.

189 4 b) Constant False Alarm Rate (CFAR) Detector

190 CFAR detectors are designed to track changes in the interference and to adjust the detection threshold to maintain
 191 a constant probability of false alarm. Since the performance of a detection scheme is measured by evaluating
 192 the probability of detection and the probability of false alarm, our strategy in analyzing a CFAR variant is to
 193 calculate its detection probability which is given by: $P_d = \int_{T} f_T(x) dx$ (10)

194 $F_Z(\cdot)$ denotes the CDF of the noise power level estimate and T is a thresholding constant required to
 195 guarantee the designed rate of false alarm. In terms of the Laplace transformation, Eq. (10) takes the form:
 196 (11) With the aid of convolution theorem, Eq. (11) can be put in another form as: $F_Z(\cdot) * F_T(\cdot)$ (12)

197 In the above formula, $M_x(\cdot)$ represents the moment generating function (MGF) of the random variable
 198 (RV) x , $Z(\cdot)$ denotes the Laplace transformation of the CDF of the RV Z , and the symbol "*" stands for the
 199 convolution process. By using Eq. (12), Eq. (11) can be written as: $F_Z(\cdot) * F_T(\cdot)$ (13)

200 The contour of integration C consists of a vertical path in the complex s -plane crossing the negative real axis
 201 at the rightmost negative real axis singularity of $M_x(\cdot)$ and closed in an infinite semicircle in the left half
 202 plane.

203 Eq. (13) demonstrates that the MGF of γ , the content of the CUT, plays an important role in determining
 204 the processor detection performance. Let's go to calculate this interesting parameter for the Swerling's models
 205 of fluctuating targets.

206 For mono-pulse application and when a nonfluctuating target return-plus-noise represents the content of the
 207 CUT, the output of this cell has a PDF given by [11]: $f(\gamma) = \frac{1}{\Gamma(M)} \gamma^{M-1} \exp(-\gamma) = \exp(-\gamma) \gamma^{M-1} / \Gamma(M)$ (14)

208 γ denotes the signal power, σ^2 is the noise power, γ/σ^2 represents the SNR at the square-law detector input
 209 and $I_0(\cdot)$ stands for the modified Bessel function of type 1 and of order 0.

210 Since the single pulse case is infrequently used, the M-pulses form of Eq. (14) is preferable. After integrating
 211 M pulses, the new form of Eq. (14) becomes [9]: $f(\gamma) = \frac{1}{\Gamma(M)} \gamma^{M-1} \exp(-\gamma) = \exp(-\gamma) \gamma^{M-1} / \Gamma(M)$ (15)

212 The MGF associated with the PDF of Eq. (15) can be easily evaluated and the result yields: $M_x(s) = \frac{1}{(1-s)^M}$ (16)

213 The unconditional MGF can be obtained by averaging the above formula over the target fluctuation distribution
 214 of γ . For χ^2 family of target fluctuation models, the RV γ is characterized by a PDF given by [18]: $f(\gamma) = \frac{1}{\Gamma(\nu/2)} \gamma^{\nu/2-1} \exp(-\gamma)$ (17)

215 The unconditional MGF is then extracted by calculating the average value of Eq. (17) given the PDF of Eq.
 216 (17). Thus, we have $M_x(s) = \frac{1}{\Gamma(\nu/2)} \int_0^\infty \gamma^{\nu/2-1} \exp(-\gamma) \frac{1}{(1-s\gamma)^M} d\gamma$ (18)

217 Eq. (18) is the fundamental formula from the Swerling's models can be derived as special cases.

227 5 Swerling I Model (SWI)

228 As Eq.(8) indicates, this model is characterized by $\gamma=1$. Replacing γ by 1 in Eq.(??8) yields: () () () ? ? ? ? ?
229 ? ? ? ? ? ? ? + = + ? ? ? ? ? ? ? ? ? ? ? + ? ? ? ? ? ? ? ? ? ? + ? = ? ? 1 1 & 1 1 1 1 1 0 M M (19)

230 In the above expression, $\bar{\gamma}$ denotes the average per pulse SNR. The substitution of this MGF into Eq.(??3)
231 results: () () ? ? ? ? ? ? ? ? ? ? ? = ? ? ? ? ? ? ? ? ? ? ? ? ? ? ? ? ? + ? ? ? ? ? ? ? ? ? ? ? + ? ? ? ?
232 ? ? ? ? ? ? ? ? ? ? ? = ? ? ? ? ? ? ? ? ? ? ? ? ? ? ? ? ? T T d d M T T T Z M M M Z M d P 1 1 1 1 1 2 2
233 1 1 (20)

234 6 Swerling II Model (SWII)

235 This model of target fluctuation has an M th degree of freedom. Setting $\gamma=M$ in Eq.(??8) leads to: () () ? ? ?
236 ? ? ? ? ? ? ? + = ? ? ? ? ? ? ? ? ? + ? ? ? ? ? ? ? ? ? ? + ? = ? 1 1 & 1 1 0 M M M (21)

237 $\bar{\gamma}$ denotes the average, over M pulses, SNR. In this case, the processor detection performance is given by: () ()
238 () () ? ? ? T d d M T Z M M M d P ? = ? ? ? ? ? ? ? ? = ? ? ? ? 1 1 (22)

239 7 Swerling III Model (SWIII)

240 This model of target fluctuation is characterized by $\gamma=2$ in the MGF of the CUT. In this situation, the MGF of
241 the concerned cell becomes: () () ? ? ? ? ? ? ? ? ? ? ? + = ? ? ? ? ? ? ? ? ? + ? ? ? ? ? ? ? ? ? ? + ? ? ? ? ?
242 ? ? ? ? ? + ? = ? ? 1 2 1 & 1 1 1 1 2 2 0 M M (23) © 2021 Global Journals () H Year 2021

243 The probability of detection of SWIII target fluctuation model will be: () () () ? ? ? ? ? ? ? = ? ? ? ? ? ? ?
244 ? ? ? ? ? ? ? ? ? ? ? + ? ? ? ? ? ? ? ? + ? = ? + ? ? ? ? ? ? ? ? ? ? ?
245 ? ? ? ? ? ? ? = ? ? ? ? ? ? ? ? ? ? ? ? ? T T d d M T T d d T T Z M M Z M M d P 2 3 3 2 2 2 1 2 1 1 (24)

246 8 Swerling IV Model (SWIV)

247 This case of target fluctuation has $(2M)$ th degrees of freedom. Thus, the substitution of $\gamma=2M$ in Eq.(??8)
248 yields: () () ? ? ? ? ? ? ? ? ? ? ? + = ? ? ? ? ? ? ? ? ? + ? ? ? ? ? ? ? ? ? ? + ? ? ? ? ? ? ? ? ? ? + ? = ? ?
249 1 2 1 & 1 1 1 1 2 0 M M M M (25)

250 Eq.(??5), as a MGF, in the definition of P_d gives the processor detection performance which has a
251 mathematical form given by: () () ? ? ? ? T T d d M T T Z M M M M M d P ? = ? ? ? ? ? ? ?
252 ? ? ? ? ? ? ? ? ? ? ? ? ? ? ? + ? = ? ? ? ? ? 1 2 1 1 2 1 2 2 (26)

253 In all cases, the false alarm probability takes a unified form; the mathematical version of which is: () () { } ?
254 ? T d d M T Z M M M fa P ? = ? ? ? ? ? ? ? ? ? ? ? = ? ? ? ? 1 1 1 (27)

255 Since enhancing detection performance of a CFAR variant is a basic requirement in evolving radar systems,
256 we choose the recent version of CFAR detectors to fulfill this objective. It is intuitive that as P_d increases, the
257 missed detection decreases and consequently, the processor performance will be enhanced. The upcoming section
258 is devoted to evaluate the performance of the linear fusion (LF) strategy to have a knowledge about its reaction
259 against fluctuating targets of Swerling models.

260 By careful examining the previous derived formulas, it is evident that they rely on the Laplace transformation
261 of the CDF of the noise power level estimate Z and its mathematical differentiation. Therefore, we are focused on
262 formulating this transformation when the detection scheme operates in an environment that has several outlying
263 targets along with the main one (ToI).

264 9 III.

265 10 Processor performance analysis

266 Specifically, the efficiency of a CFAR scheme is measured in the perfect case of operating conditions or in the
267 presence of some of fallacious targets beside the ToI. Since the ideal situation is a special case of nonideal
268 operation, it is preferable to analyze the processor performance in heterogeneous background. This is actually
269 the case that we are going to follow in the upcoming subsections.

270 11 a) Single Adaptive Processors

271 This procedure of CFAR technology performs robustly in both inhomogeneous clutter and target multiplicity
272 situations. It extracts the K th largest sample from the candidates of the reference window to represent the
273 estimate of the unknown noise power. To carry out such extraction, it ranks the reference cells in an ascending
274 order, in such a way that: $1, \dots, \dots, \dots, 2, 1$ & 1 () (? = + ? N y y ? ? ? (28) () N K y Z K OS ? ? ? 1 &

275 In this ranked samples, $y(1)$ denotes the lowest noise level whilst $y(N)$ represents the highest one. After
276 the rank order, we plan to pick the sample of K th level to constitute the unknown noise level in the reference
277 window. Thus, the OS test-statistic takes the form:

278 12 i. Ordered-Statistics (OS)

279 Aiming at evaluating the performance of the OS algorithm, this necessitates the PDF calculation of the K th
280 ordered sample in the case where the samples are independent, but not identically distributed. To accomplish

281 such objective, let us consider that the reference window has "R" cells that contain outlying target returns each
 282 with power level $\gamma(1+\gamma)$ and the remaining, "N-R" ones having thermal noise only with power level γ . In both
 283 cases, the observations are governed by the exponential PDF and are statistically independent quantities. Taking
 284 these assumptions into account, the cumulative distribution function (CDF) of the K th ordered cell is given by
 285 [19]: $(\cdot)(\cdot)(\cdot)(\cdot)\{\cdot\}(\cdot)\{\cdot\} m R I j n j i m n R N C m n N K i R N i M i n R i M a x j N H K t F t F m j i n j j i$
 286 $R j R N R N t F \gamma = \gamma = \gamma ? = \gamma ? = \gamma ?$
 287 $? ? ? ? = \gamma ? ? ? 1 1 1 1 , ; 0 0) , () , 0 ((30)$

288 In the above expression, $F_C(\cdot)$ represents the CDF of the cell that contains clutter background whilst $F_I(\cdot)$
 289 denotes the same thing for the cell that has interfering target return. The random variable (RV's) representing
 290 the returns from clutter background has MGF of the same form as that given in Eq.(??8) after nullifying γ . By
 291 using the resulting form of that equation, the Laplace transformation of $F_c(\cdot)$ becomes: $(\cdot)(\cdot) ? + ? ? ? = ? 1$
 292 $M C (31)$

293 The Laplace inverse of the above formula yields: $(\cdot)(\cdot)(\cdot) t U t e t F t M C ? ? = ? + \hat{I} ? ? ? = 1 0 1 1 ? ? ?$
 294 (32) Where $(\cdot) ? ? ? ? ? ? ? ? ? ? ? ? ? ? + ?$
 295 $? ? ? 1 1 2 2 1 1 1 ? ? ? ? ? ? ? ? ? ? ? ? ? ? (34)$ and $(\cdot)(\cdot) ? ? = ? ? ? ? M j k k j k j k j j 1 2 2 1 1 ? ? ? ? ? ? ?$
 296 (35)

297 The substitution of Eqs.(32 & 33) into Eq.(30) leads to: For the interference case, there are two situations: a.
 298 $\gamma 2$ fluctuation with 4-degrees of freedom: if the interfering target fluctuates following this statistical type, F_I
 299 (\cdot) has a form given by [12]: $(\cdot) ? ? ? ? ? ? = ? ? ? ? = ? ? = ? ? = ? ? ? ? ? ? + ? ? ? ? ? ? + \hat{I} ? ? ?$
 300 $? ?$
 301 $t M m m k i j k j i R N i R i j N H K e e F n t m t j i k j j i R j R N R N t 1 1 0 0 0) , \min(\cdot) , 0 \max(\cdot) 1 (\cdot) 1$
 302 $(\cdot) , ; (? ? ? (\cdot)(\cdot) 2 1 1 ,) (1 1 1 1 1 2 2 1 ? + ? + ? = ? ? ? ? ? ? ? ? ? ? +$
 303 $? ? = ? = ? ? ? + ? t U t i t e L F t M M i i I (33)$

304 By using binomial theorem, we can expand the bracketed quantities as a binomial of t. This expansion results
 305 in reformatting Eq. (36) as: $? ? ; ((\cdot)(\cdot)(\cdot) ?$
 306 $+ \hat{I} ?$
 307 $? ? ? ? ? ? ? ? = ? ? ? ? ? ? ? ? ? ? + ? ? = ? ? = ? ? = ? ? = = = ? = ? = ? ? = ? ? = ? ? = ? ?$
 308 $= ? = ? ? = ? = ? t R N t R R R N j i j j i R j R N R N t n M n n n R M M R R R M R M M N K i R N R$
 309 $N R N i j j i R N i R i j N H K M M M M F ? ? ? ? ? ? ? ? ? ? ? ? ? ? \mu ? ? ? \mu \mu ? ? ? ? 1 0 1 2 1 2 0 1 1 ? ? ? ? ?$
 310 $? ? ? ? ? ? (37)$

311 The Laplace transformation of Eq. (37) gives: $? ? ; ((\cdot)(\cdot)(\cdot) ? ? ? ? ? ? ? ? + + ? ? + ? ? ? ? ? ? ? ? ? ?$
 312 $? ? ? ? ? ? ? ? ? ? = ? ? ? ? ? ? ? ? + + ? ? \hat{I} ? ? ? ? ? ? ? ? ? ? ? ? ? ? + \hat{I} ? ? ? ? ? ? ? ? ? ? ? ? ? ?$
 313 $= ? = ? ? ? ? ? ? ? ? ? ? ? ? ? ? + + ? ? ? = ? ? = ? ? = ? ? =$
 314 $= = = ? ? = ? ? = ? ? = ? ? = ? ? = ? ? = ? ? = ? ? = ? ? = ? ? = ? ? = ? ? = ? ? = ? ? = ? ? = ? ? = ? ? =$
 315 $N M M M M R M M M R R R M R M M N K i R N R N R N i j j i R N i R i j N H K ? ? ? ? 1 0 1 2 1 2 0 1 1 1$
 316 $1 0 1 2 1 0 0 0 0 0 2 1 0 1 0 1 0 0 0 0 0) , \min(\cdot) , 0 \max(\cdot ? ? ? ? ? ? ? ? ? ? ? ? ? ? (38)$

317 In the previous formulas, the term $(J; j_1, j_2, \dots, j_M)$ is defined as [20]: $s(\cdot)(\cdot)(\cdot) ? ? ? ? ? ? ? ? ? ? ? ? =$
 318 $+ \hat{I} ? ? ? ? ? ? + \hat{I} ? ? = = M M M i i M J j i f J j i f j j j j J J 1 1 1 2 1 0 1 1 , \dots, , ; ? ? ? ? (39) (\cdot) ? ? ? ?$
 319 $? ? ? ? ? ? ? ? + ? ? ? ? ? ? ? ? + ? ? = ? = ? 1 1 \& 1 1 1 M I L F t (40)$

320 y evaluating the Laplace inverse processing of the above formula, one obtains: $(\cdot)(\cdot)(\cdot) ? ? ? = ? ? ? ? =$
 321 $M j i i j j i j M j j j I t U t t ? ? ? (41)$

322 The substitution of Eqs.(32 & 41) into Eq.(30) yields: $? ? ? ? ? = ? = ? ? ? ? = ? ? = ? ? = ? ? = ? ? ? ? ?$
 323 $? ? ? ? ? ? ? ? + \hat{I} ?$
 324 $R M n t n N K i R N t M m m i j j i R N i R i j N H K e e F n m t j i j j i R j R N R N t 1 1 0 0 0) , \min(\cdot) , 0$
 325 $\max(\cdot) 1 (\cdot) 1 (\cdot) , ; (? ? ? ? ? ?$

326 With the aid of binomial theorem, the bracketed quantities can be expanded as a binomial of t. Following this
 327 procedure of expansion, Eq.(??2) can be rewritten as: The Laplace transformation of Eq.(??3) results: $? ? ; (($
 328 $(\cdot)(\cdot)(\cdot)(\cdot) [(\cdot)(\cdot) ? ? ? ? ? ? ? ? + ? ? ? ? ? ? + \hat{I} ?$
 329 $? ? ? ? ? ? ? ? ? ? ? ? ? ? = = ? ? = ? = ? = = ? = ? ? = ? ? = ? ? = ? ? ? = = = ? ? = ? = ? ? ? ? ? ?$
 330 $? ? ? ? ? ? ? ? M n n n u R v R v R v M v M M u M R N u R N u R N u i j j j N K i R N i R i j N H K t v R$
 331 $N t v v v R u u u u R N j i j j i R j R N R N t M M M F 1 0 0 0 1 2 1 1 0 1 2 1 0 0 0 0 0) , \min(\cdot) (\cdot) (\cdot) (\cdot)$
 332 $[] (\cdot) (\cdot) ? ? ? ? ? ? ? ? + ? ? + ? ? ? ? ? ? ? ? ? ? ? ? ? ? ? ? ? = ? ? ? ? ? ? ? + ? \hat{I} ? ? ? + \hat{I} ? ? ? ? ? ? ? ? ? ?$
 333 $? ?$
 334 $? ? ? = ? ? = ? ? = ? ? ? = = = ? ? = ? = ? M n n n u v v v R u u u u R N j i j j i R j R N R N v R N M$
 335 $M M u M R v R v R v M v M M u M R N u R N u R N u i j j j N K i R N i R i j N H K 1 1 \dots 1 1 0 0 0 0 1 2 1$
 336 $1 0 1 2 1 0 0 0 0 0) , \min , 0 \max 1 0 1 2 1 1 0 ? (44)$

337 Once Eqs. (38 & 44) are obtained, the false alarm and detection performances are completely evaluated, as
 338 Eqs. (20, ??2, ??4, ??6, ??7) demonstrate. The major drawback of this scheme is the high processing time that
 339 is taken in performing the sorting mechanism.

340 The trimmed-mean (TM) algorithm is the more generalized version of the OS scheme. It may be considered
 341 as an amended version of the OS scenario. The motivation of using this algorithm is to combine the benefits of
 342 averaging and ordering along with censoring. In this scheme, the noise power is estimated by a linear combination
 343 of some selected ordered range samples.

344 The linear combination may be anticipated to give better results because averaging estimates the noise power
 345 more efficiently as in the case of the CA processor and thus loss of detection in uniform background is more
 346 tolerable. In the TM-CFAR detector, the lowest L_1 ordered range samples and the highest L_2 ordered ones are
 347 excised before summing the remaining cells to formulate the statistic Z_{TM} . Thus, $(\cdot)(\cdot) \dots + = ? 2 1 1 2 1 ,$
 348 $L N L T M y Z L L ? ?$ (45)

349 Clearly, the ordered samples $y(i)$'s are neither independent nor identically distributed, so the performance
 350 evaluation of TM scheme becomes cumbersome. To handle this evaluation, a new linear transformation is needed.
 351 In other words, the following transformation can be used to make the ordered samples $y(i)$'s satisfy the IID
 352 property [18]. Mathematically, this transformation takes the form: $(\cdot)(\cdot)(\cdot) 2 1 1 1 ? ? ? ? + + ? ? ? ? U y y$
 353 $Y L L$ (46)

354 As a function of these new variables Y_i 's, Eq. (??5) can be rewritten as: © 2021 Global Journals ii. Trimmed-
 355 Mean (TM) $(\cdot)(\cdot) 2 1 1 2 1 \& 1 , L L N L j L L L T L j T j T T M Y Z ? ? ? + ? = ? =$ (47) $(\cdot)(\cdot)(\cdot) ? ?$
 356 $? ? ? ? ? ? < ? ? = ? = ? ? ? ? ? ? + + + T N H j L N H j L N H L L j$ for $R N R N j$ for $R N Y M j 1 , ; , ; 1$
 357 $, ; 1 1 1 1 1$ (48)

358 After obtaining the formula (48), the computation of the MGF of the noise level estimate Z_{TM} becomes an
 359 easy task owing to the independency of its samples. Thus, $(\cdot)(\cdot)(\cdot) ? + ? = ? ? = ? ? = 1 , ; 1 2 1 ? ? ? T L L$
 360 $Y L L Z T T M M M$ (49)

361 Though the TM-CFAR scheme offers good performance, the large processing time, which is taken in ordering
 362 the candidates of the reference window, limits its practical applications. This problem can be overcome by
 363 partitioning the reference window into Q , symmetrical or nonsymmetrical, smaller sub-windows. The samples in
 364 the each sub-window are processed and its statistic Z may be estimated according to a specified rule and the final
 365 statistic is chosen by further processing the Q sub-window outputs. Here, we apply this idea by symmetrically
 366 partitioned the reference window into preceding and succeeding sub-windows ($Q=2$). In this situation, suppose
 367 that the preceding subset has R_1 cells from outlying target returns, $N/2-R_1$ ones from thermal background, the
 368 lowest P_1 cells and the highest P_2 ones are censored from its ordered statistic before adding the remaining cells
 369 to establish the background level of the preceding sub-window. Similarly, assume that the succeeding sub-window
 370 has R_2 cells of fallacious target returns, $N/2-R_2$ samples containing clutter, its associated ordered-statistic is
 371 trimmed from its ends, where the lowest S_1 ordered cells are excised and S_2 highest ranked cells are nullified.
 372 Under these circumstances, the MGF's of their noise power level estimates, Z_1 and Z_2 , have the same form as
 373 that given by Eq. (??9) after replacing its common parameters with their corresponding values for the preceding
 374 and succeeding subsets. Since the meanlevel (ML) operation represents the simplest way that uses arithmetic
 375 averaging to extract the unknown noise power level, the two noise level estimates are combined through the ML
 376 operation to formulate the final noise power estimate. Mathematically, this can be expressed as: $(\cdot) 2 1 , Z Z$
 377 $Mean Z f =$ (50)

378 Since the two noise level estimates are statistically independent, the final noise level estimate has a MGF given
 379 by: $(\cdot)(\cdot)(\cdot) 2 1 2 1 , ; , ; S S Z P P Z Z M M M T M T M f ? ? = ?$ (51)

380 As Eqs. (20, ??2, ??4, ??6, ??7) indicate that the probabilities of detection and false alarm are functions of
 381 the Laplace transformation of the CDF of the noise level estimate Z_f , it is necessary to compute such important
 382 parameter. As a function of the MGF of Z_f , its CDF has a Laplace transformation given by [21]: $(\cdot)(\cdot) ? ? ?$
 383 $= ? M Z Z f f$ (52)

384 Once the s -domain representation of the PDF of the resultant noise level estimate is formulated, the processor
 385 false alarm and detection performances can be completely evaluated, as we have proved in the previous section.
 386 It is of importance to note that the TM scenario reduces to the conventional CA and OS algorithms for specific
 387 trimming values. In other words, TM (0, 0) and TM (K-1, N-K) tend to the well-known CA and OS (K)
 388 processors, respectively; each handles N reference cells to estimate the unknown noise power level. Thus, for the
 389 conventional CA and OS (K) schemes, we have:

390 In terms of the s -domain representation of the CDF of the ordered samples $y(i)$'s, the MGF of the random
 391 variables Y_j 's can be easily calculated as [12]: $(\cdot)(\cdot)(\cdot) 0 , 0 ; 0 , 0 ; ? ? = ? M M M Z Z Z T M T M CA$ (53)
 392 and $(\cdot) ? ? ? ? ? ? ? ? ? ? ? ? ? ? ? ? ? ? = ? 2 2 1 1 2 , 1 ; 2 , 1 ; K N K Z K N K Z Z M M M T M T M OS$
 393 (54)

394 In Eq. (??3), the noise levels extracted from the preceding and succeeding sub-windows of the OS scheme are:
 395 $(\cdot) ? ? ? ? ? ? ? ? ? ? 2 \dots, , 2 , 1 , , \& 2 1 2 1 2 1 N K K K K y Z y Z$ (55) iii. Cell-Averaging (CA)

396 The CA is the king of the CFAR schemes that has the highest homogeneous performance, given that the clutter
 397 is exponentially distributed and the contents of the reference window are IID. It uses the maximum likelihood
 398 estimate of the noise power to set the adaptive threshold. The CA performs the traditional averaging technique
 399 by dividing the summing of the contents of the reference cells by their number. Commonly, it is regarded as
 400 the reference model against which new implementations are compared. Nevertheless, it exhibits a weak behavior
 401 against heterogeneous background which are frequently created by clutter edges and the appearance of multiple
 402 target situations. If one or more spurious targets fall within the reference window, the probability of losing the
 403 targets will be increased owing to the severe phenomenon of target masking.

404 Since CA is a special case of TM scheme, we can exploit the analysis of the TM variant to evaluate the
 405 performance of the CA detector, where all of its ordered samples are activated. Thus, under the same conditions
 406 of the double-window TM scenario, the MGF of the double-window CA processor is given by Eq.(53).

13 b) Combined CFAR Schemes i. Linear Fusion (LF) Emerged Strategy

A robust detector should not only pick out targets but also diminish false alarms. For target detection in complex background, it is difficult to realize high level of detection simultaneously with holding low rate of false alarm. Therefore, an effective detector dictates an incorporation of different features in such a way that each aspect resolves one of the challenges that enface the detection characteristics. In other words, an architecture involving decentralized processing at multiple sensor locations provides the proper choice of optimum results in heterogeneous situation. From this point of view, the fusion strategy has rapidly become a methodology of choice for detecting fluctuating targets. Such establishment involves higher reliability and survivability, along with improved system performance at low latency. In this scenario of CFAR technology, a CA scheme provides a low false alarm rate and a high level of detection, its output is taken as a baseline for the fusion center. When the CA output is positive (presence of target), there is a possibility of occurrence of false alarm, caused by clutter transition or target multiplicity. To eliminate this eventuality, the AND fusion Rule(I), indicated in Eq.(56), can be applied. This rule necessitates the application of an AND logic between the CA output and that obtained by applying an OR logic between the outputs of OS and TM schemes. On the other hand, when the CA output is negative (absence of target), there exists the possibility of a target lost caused by clutter interference. To avoid such occurrence, an AND fusion Rule(II), exhibited in Eq.(57) is utilized. This involves the application of an AND logic between the outputs of OS and TM variants. OS II TM OS CA I Rule (56)

In the previous expression, "OR" stands for the algebraic Boolean of OR gate whilst "AND" represents the same thing of AND gate. Since the occurrence of one of them excludes the occurrence of the others, they are mutually exclusive. Taking into account that the decisions of CA, OS, and TM approaches are independent events, the global detection probability "P LF" of the new implementation can be obtained by summing the outcomes of these rows. Thus, P LF has a mathematical form given by: $P_{LF} = P_{CA} + P_{OS} + P_{TM} - P_{CA}P_{OS} - P_{CA}P_{TM} - P_{OS}P_{TM} + P_{CA}P_{OS}P_{TM}$ (57)

Here, P miss denotes the probability of missed detection. All the parameters of Eq.(57) are previously calculated. So, the detection performance of the LF-CFAR strategy is completely analyzed.

Our scope in the upcoming section is to numerically simulate the derived formulas through a PC device using C++ programming language to see the new contribution of the LF style in the CFAR world.

14 IV. Simulation results and Discussion

It is of importance to numerically evaluate the performance of the examined model. This section introduces the simulation results in order to confirm the performance superiority of the proposed algorithm. How well the model reacts against the presence of inhomogeneous background, can be assessed by several parameters. The most dominant and common ones include detection performance, CFAR loss, and actual probability of false alarm which measures the model's capability of holding the rate of false alarm stationary en face of outliers. Thus, we go to compute the detection performance, in the absence as well as in the presence of fallacious targets, for two and four (M=2 & 4) post-detection integrated pulses to see to what extent the pulse integration can ameliorate the reaction of the CFAR scheme against fluctuating targets. In our simulated results, it is assumed that the reference window has a size (N) of 24 cells, the designed P fa is 10^{-6} . For OS scenario, the 10th ordered sample, OS (10), is chosen to represent its noise level estimate of each reference sub-window, whilst for TM scheme, the two smallest cells along with the two highest ones, TM (2,2), are excised from the ordered set of each sub-window before adding the remaining ordered samples to extract its background power. Since the double-windows and mean-level operation are common for all the CFAR processors under test, it is of preferable to omit these features from nominating them. Instead, it is sufficient to designate each one of them with the CFAR rule used in estimating the unknown noise level of each sub-window as CA, OS (10) and TM (2,2). Fig. (2) shows the level of detection as a function of primary target signal strength (SNR) of the new methodology in homogeneous environment for the four Swerling models when the CFAR circuit based its decision on integrating two (M=2) consecutive sweeps. For the sake of comparison, the single sweep (M=1) case is attached for 2 fluctuating target with two (?=1) and four (?=2) degrees of freedom. Additionally, the same results of the optimum (N-P) detector are included among the curves of Fig. (2). In the case of single pulse operation, the displayed results illustrate that there is a turnover point; below which the N-P scheme surpasses, in detection performance, the LF strategy whilst upper this point the reverse is occurred. In other words, when the target signal is strengthened, the detection performance of the new variant outweighs that of the N-P detector and the gap between the two curves increases as the signal becomes more strengthened. Moreover, the processor performance for fluctuating targets with ?=2 is higher than that obtained for ?=1 and this behavior is noticed for LF and N-P processors given that the turnover point is exceeded. Furthermore, the performance of SWI model coincides with that of SWII model and the performances of SWIII and SWIV models are the same.

For M=2, on the other hand, it is noted that the turnover point is shifted towards lower signal strength. At the preceding of this point, SWI has the top performance whereas SWIV gives the worst detection level. As this point is surpassed, the reverse is observed; where SWIV model has the highest performance whilst the SWI model exhibits the lowest probability of detection. It is of importance to note that the detector performance against SWII fluctuation model coincides with that corresponds to SWIII model in the case where the radar receiver has

468 a non-coherent integration of two successive pulses ($M=2$) as Eq.(8) demonstrates. As we have noticed for $M=1$,
469 the N-P detector has a detection performance which is meagerly superior, at lower SNR, than that of LF scheme,
470 when the turnover point is not reached. When the SNR is greater than that corresponding to the turnover
471 point, the new methodology has the top performance whatever the fluctuation model is. The gap between the
472 two curves (LF & N-P) corresponding to SWI model is the widest whereas this gap is narrow for SWIV model,
473 taking into account that the LF strategy has always the top performance against any fluctuation model. ??)
474 on the exception that the operating environment is contaminated with some interfering targets instead of being
475 free of them. The results of this scene are obtained on the assumption that one of each reference sub-window
476 cells contains interfering target return ($R_1 = R_2 = 1$); the signal strength of which equals to that of the primary
477 target ($INR=SNR$) and follows the same Swerling model, as the target of interest, in its fluctuation. A big
478 insight on the variation of the curves of this plot indicates that the turnover points of LF and N-P are different,
479 instead of coincide as in homogeneous case in Fig. (2), and this occurs either the pulse integration is absent
480 ($M=1$) or present ($M=2$). In addition, the N-P detector has the top performance especially when the signal
481 strength is modest. As the target echo becomes strengthened, the detection performance of the new processor
482 approaches that of the N-P and may surpass it if the CFAR circuit is provided by pulse integration, as Fig. ??3)
483 demonstrates. Moreover, the point of exceeding for SWI fluctuation model takes place at a SNR which is lower
484 than that occurs for SWII model which in turn precedes, in its location, that associated with SWIV model. It
485 is of importance to note that this behavior doesn't appear if pulse integration doesn't achieve. The single sweep
486 performance confirms this knowledge.

487 Fig.(??) repeats the behavior of LF and N-P, against fluctuating targets, when the operating environment is
488 ideal (homogeneous) as that displayed in Fig. (2) with the exception that the radar receiver builds its decision
489 on integrating four ($M=4$), instead of two ($M=2$), successive pulses. The portrayed results of this figure prove
490 that the candidates of this figure have the same variation as those corresponding in Fig. (2) within some gain.
491 Additionally, the gap between the performance of novel scheme and that of N-P becomes evident; with LF
492 detector always on the top given that the signal strength exceeds the turnover point.

493 Similarly, Fig. ??), the current results exhibit some noticeable remarks as: the gap between the LF performance
494 and optimum (N-P) is narrower, the point of exceeding is shifted towards lower SNR with the same sequence of
495 Swerling models as that outlined during our comments on the curves of Fig. ??3), and there is an evident gain
496 in the performance of the examined and standard detectors. Now, Let us go to evaluate another figure of merit
497 which is known as CFAR loss. Fig. (6) shows how the signal strength must be to satisfy a detection level of 90%
498 ($P_d = 0.9$) as a function of the correlation strength among the primary target returns when this target obeys ?
499 2 -statistics, with two ($?=1$) degrees of freedom, in its fluctuation. As a reference of comparison, the traditional
500 CFAR and N-P schemes are incorporated among the results of the LF style. The displayed results are acquired on
501 the assumption that the environment of operation is ideal and two ($M=2$) consecutive sweeps are non-coherently
502 integrated. A big insight on the behavior of the curves of this figure demonstrates that as the correlation among
503 the target returns increases, the echo signal must be more strengthened to reply the required level of detection.
504 Additionally, the conventional OS scenario needs the highest, relative to the other ones stated here, signal power
505 to attain 90% level of detection, the standard TM mechanism comes next, the traditional CA procedure reserves
506 the third position, the optimum (N-P) occupies the fourth location, whilst the new methodology (LF) needs the
507 minimum signal strength in order to accomplish the requested probability of detection. The results of this scene
508 reveals the superiority of the underlined detector over its original ones as well as the N-P which is taken as a
509 reference of any new variant added to the CFAR world. Fig. (7) depicts the same behavior for the concerned
510 processors when the primary target fluctuates in accordance with ? 2 -statistics, with four ($?=2$) degrees of
511 freedom. The tested variants follow the same sequence, as indicated in Fig. (6), in demanding the signal strength
512 to reply a detection level of 90%. Moreover, for any one of the examined schemes, the signal power required in
513 this situation is weaker than that needed in Fig. (6) to satisfy the same probability of detection.

514 In multiple target situations, Figs. (8)(9)(10)(11) illustrate the needed signal strength to satisfy a given level of
515 detection when the primary and the secondary targets follow SWI, SWII, SWIII, and SWIV models, respectively,
516 in their fluctuation for the underlined detectors given that the decision is carried out based on integrating two
517 ($M=2$) successive pulses and the outlying target returns have the same signal strength as those of primary target
518 ($?=?$).

519 As a reference of comparison, the results of the N-P scheme are included among the curves of these figures
520 under the same target fluctuation model. Fig. (8) portrays the required signal power versus the preassigned level
521 of detection for the standard as well as the derived versions when one cell among the contents of each reference
522 sub-window is contaminated with extraneous target returns ($R_1 = R_2 = 1$). The displayed results illustrate
523 that the CA technique can reply the request probability of detection till a specified level beyond which it hasn't
524 the capability to satisfy the needed level of detection whatever the signal strength is. In this regard, we define
525 the dynamic range as the range belong to which, the CFAR processor can reply any given level of detection.
526 Based on this definition, the CA scheme has a limited dynamic range which is very narrow. All the other under-
527 examination processors are able to reply any level of detection with different signal powers. For lower values of
528 detection probability, there is a gap between the signal strengths needed by LF strategy and N-P detector with
529 LF needs the highest. However, as the pre-assigned detection level increases, this gap becomes narrower till the
530 two curves coincide and may LF requests the lowest signal strength to verify the high levels of detection. The

OS (10), TM(2, 2), and LF scenarios have full dynamic range, with OS(10) demands the highest whilst LF needs the lowest signal power to give the pre-assigned level of detection. In addition, the length of the dynamic range of CA detector varies as a function of the target fluctuation model in such a way that SWI model gives smallest whilst SWIV model results in relatively the largest extend of the dynamic range. The remaining schemes have always the full length for their dynamic range irrespective the fluctuation model is. However, the required signal strength varies depending on the model of fluctuation in such a way that the SWI model requires the highest whereas the SWIV model needs the lowest signal power to reply the same level of detection.

Finally, we are going to test the capability of the new methodology of holding the rate of false alarm unchanged en face of fallacious target returns that may exist among the contents of the reference sub-windows. This category of plots includes Figs. 12 & 13). While Fig. (12) is devoted to measure the actual false alarm rate, as a function of the correlation strength among the interferer's returns, in the case where the outliers fluctuate following χ^2 -distribution with two-degrees ($\nu=1$) of freedom, Fig. (13) depicts the same thing for χ^2 -distribution with four-degrees ($\nu=2$) of freedom for the fluctuation of the interferers. In these two figures, it is assumed that each reference sub-window has only one contaminated cell ($R_1 = R_2 = 1$) and the interference strength has a power of 10dB ($\rho=10$ dB). In addition, the data of these figures is established taking into account that the CFAR circuit non-coherently integrates two successive pulses ($M=2$). The displayed results of Figs. 12 & 13) demonstrate that the LF derived version has the ability of maintaining the false alarm rate, as the standard OS (10) and TM(2, 2) procedures, whatever the strength of correlation among interferer's returns is. As predicted, the conventional CA detector is incapable of fixing the rate of false alarm against the existence of outlier's returns.

V.

15 Conclusions

According to the analysis outlined above, the current investigation is aimed at comparing the performance of several CFAR alternatives regarding the maintaining of the false alarm probability and the reaching of the top of detection probability with the goal of selecting the most promising CFARs. For the Swerling target models, embedded in white Gaussian noise of unknown level, we derive an analytical expression for the overall probability of detection while the overall probability of false alarm is retained at the desired level for the given fusion rules. Through extensive simulations, the superiority and robustness of the linear fusion mechanism are clearly demonstrated by outperforming the conventional processors of CA, OS, TM and N-P in scenarios with different target fluctuation models, different correlation strengths among the target's returns, different numbers of integrated pulses, and varied operating circumstances. This ability to obtain improved performance compared to existing models is the major contribution of this work. In other words, performance analysis, conducted on both analytical and simulated results, highlights that the new architecture operating in multi-target background guarantees the constant false alarm rate property with respect to the correlation strength variations and a limited detection loss with respect to the other detectors, whose detection thresholds nevertheless are very sensitive to the interference power. The cost is that LF-CFAR suffers from more computational burden and elapsed time than other processors. We conclude from our simulation results that the fusion detector has higher quality detection interactions in heterogeneous environments. In other words, the linear fusion enjoy significant advantages in both the false alarm regulation property and detection performance, as the displayed results of

¹Multi-Target Detection Capability of Linear Fusion Approach under Different Swerling Models of Target Fluctuation

²() H © 2021 Global Journals Year 2021 Multi-Target Detection Capability of Linear Fusion Approach under Different Swerling Models of Target Fluctuation

³() H Year 2021 Multi-Target Detection Capability of Linear Fusion Approach under Different Swerling Models of Target Fluctuation

⁴() H © 2021 Global Journals

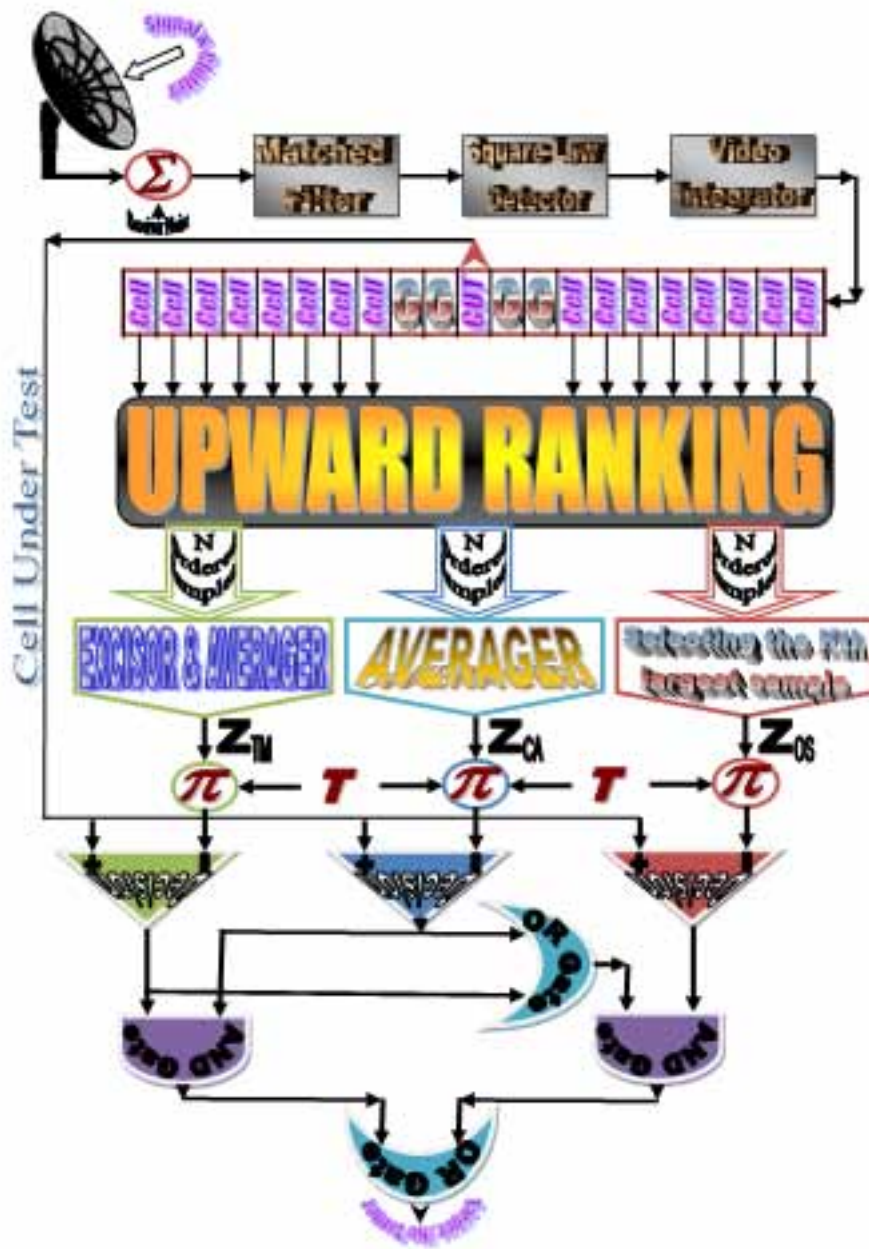


Figure 1:

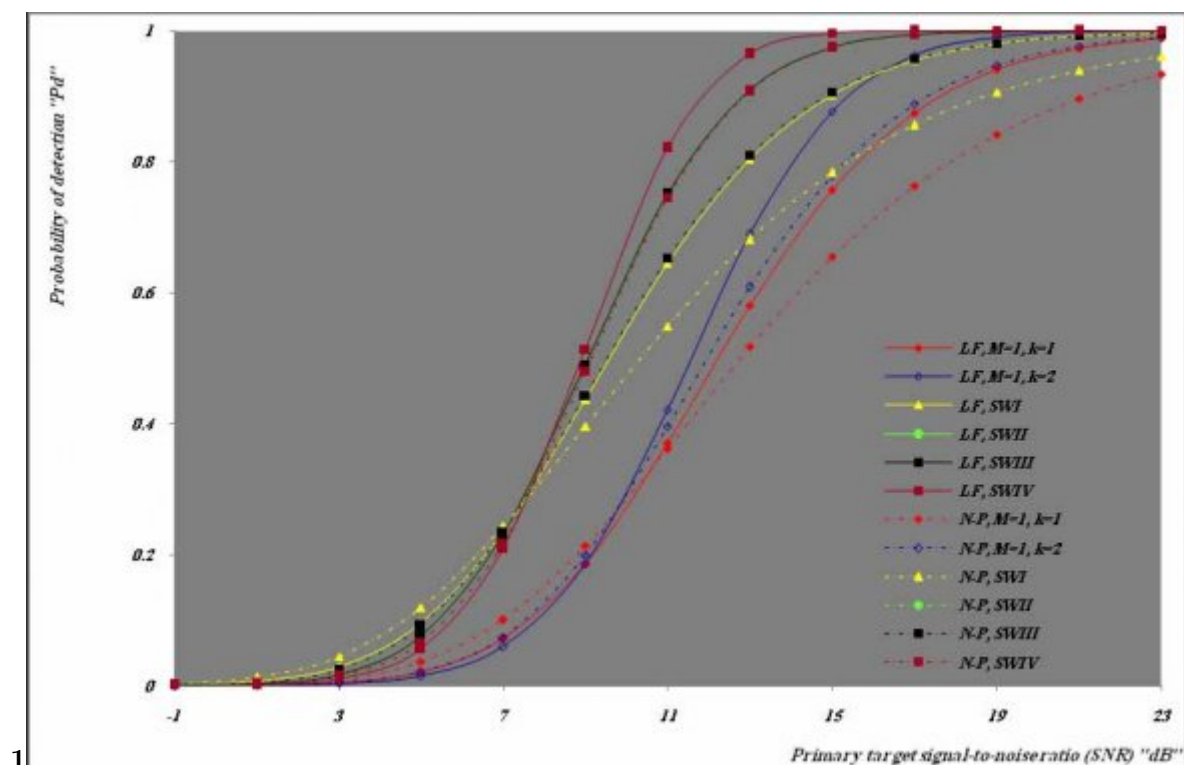


Figure 2: Fig.(1)

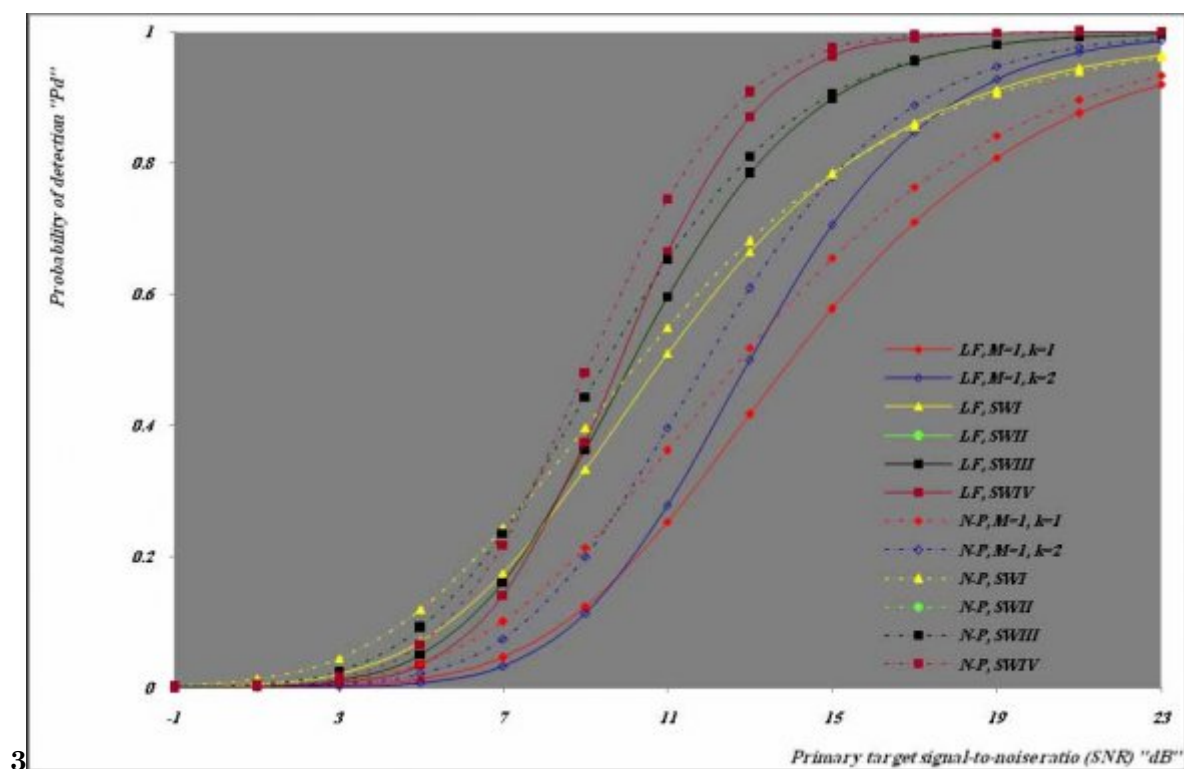


Figure 3: Fig.(3)

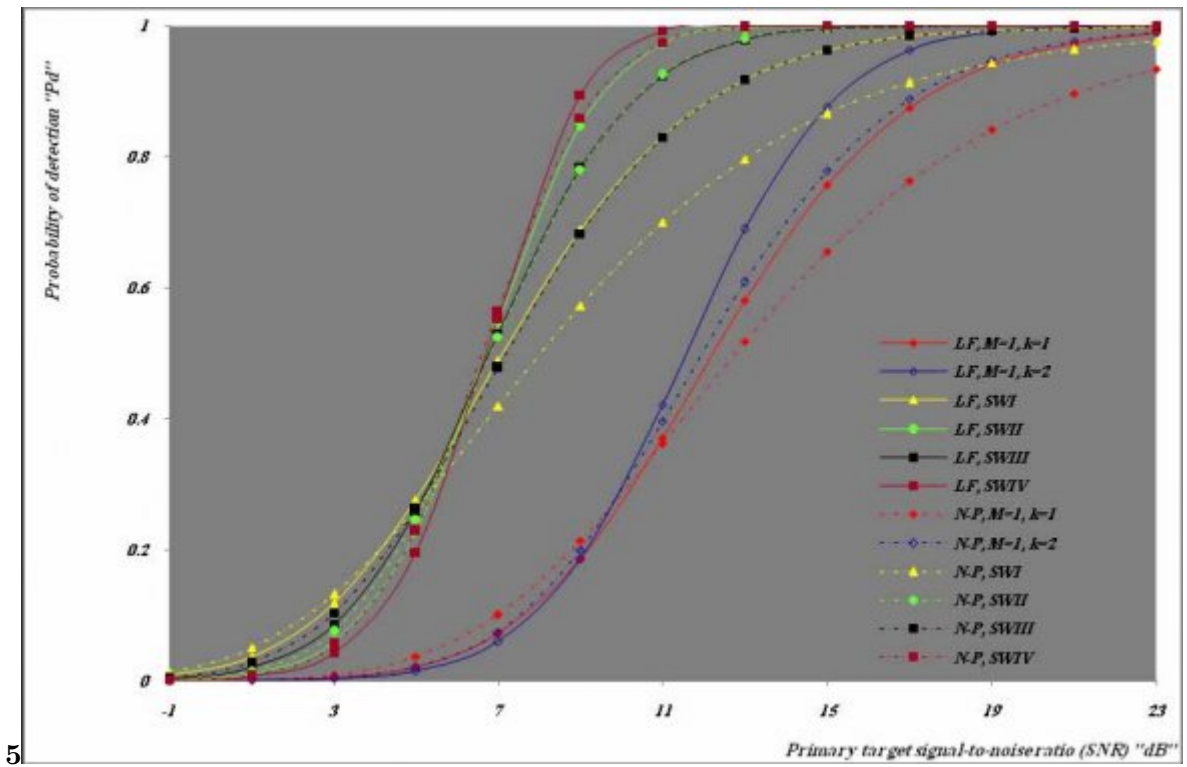


Figure 4: (5)

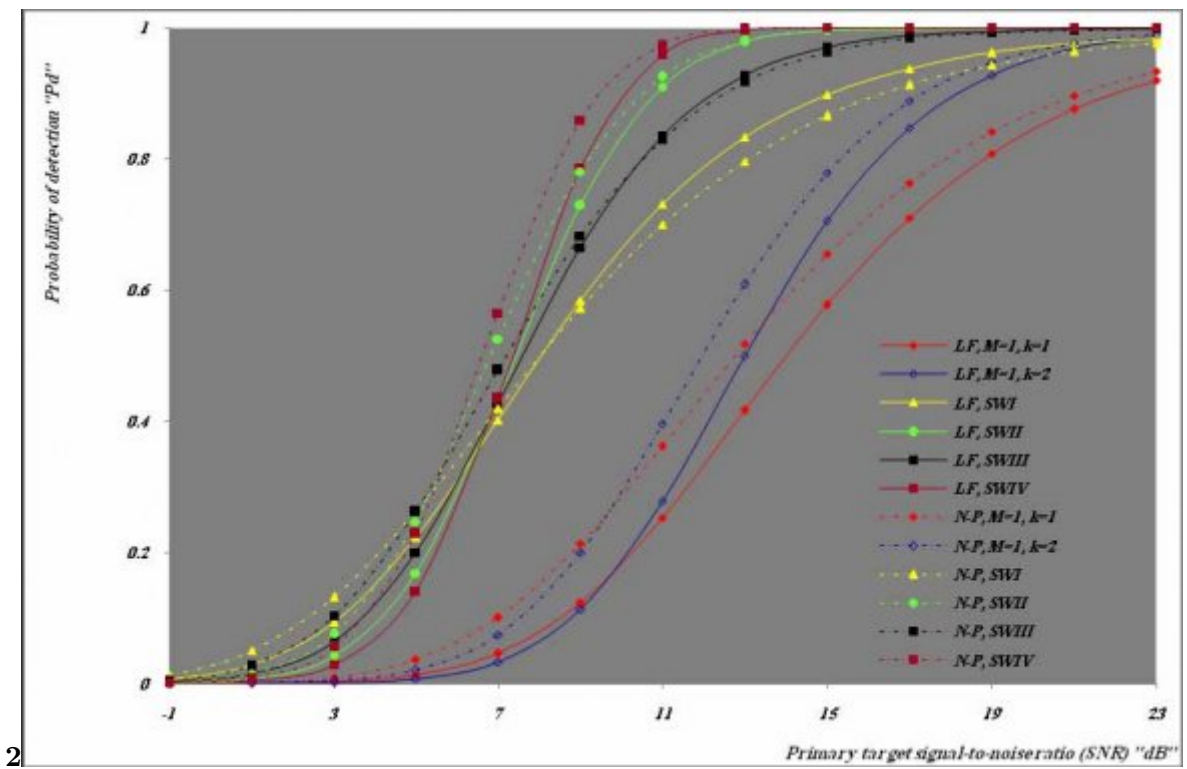


Figure 5: Fig. (2)

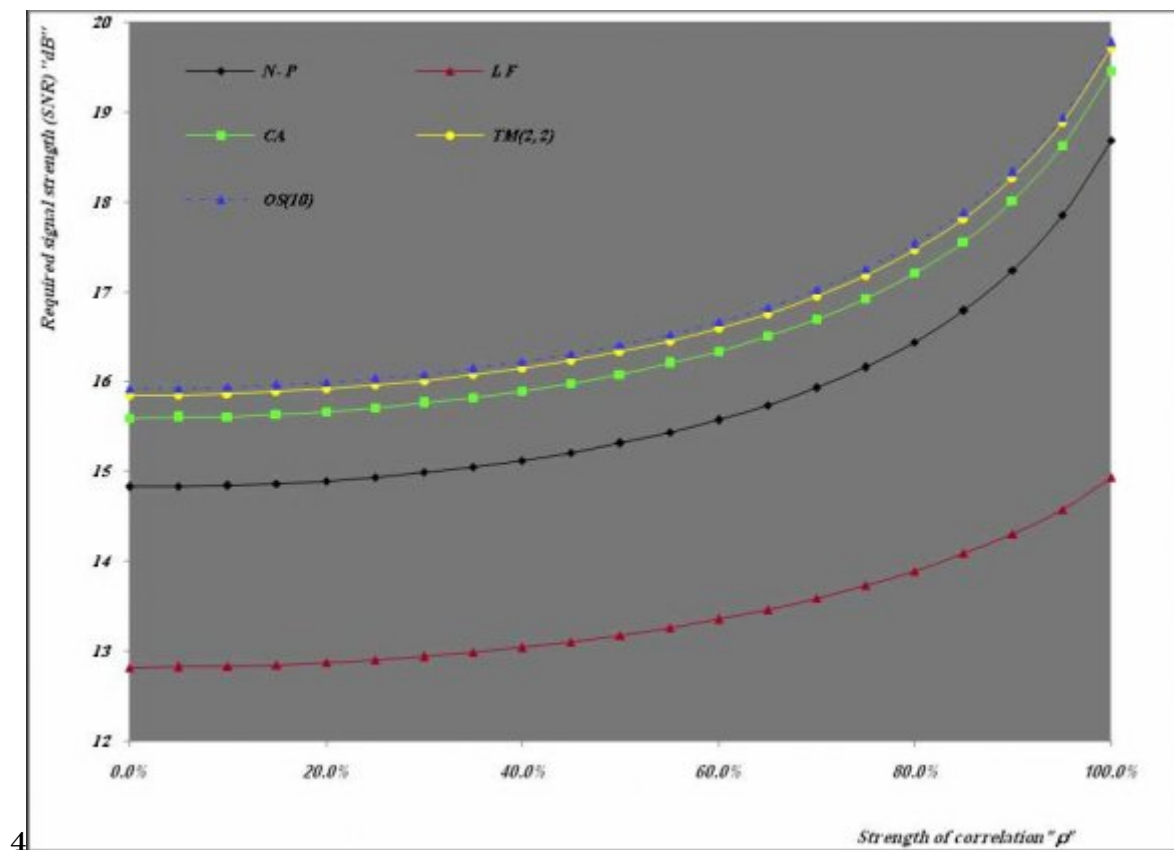


Figure 6: Fig. (4

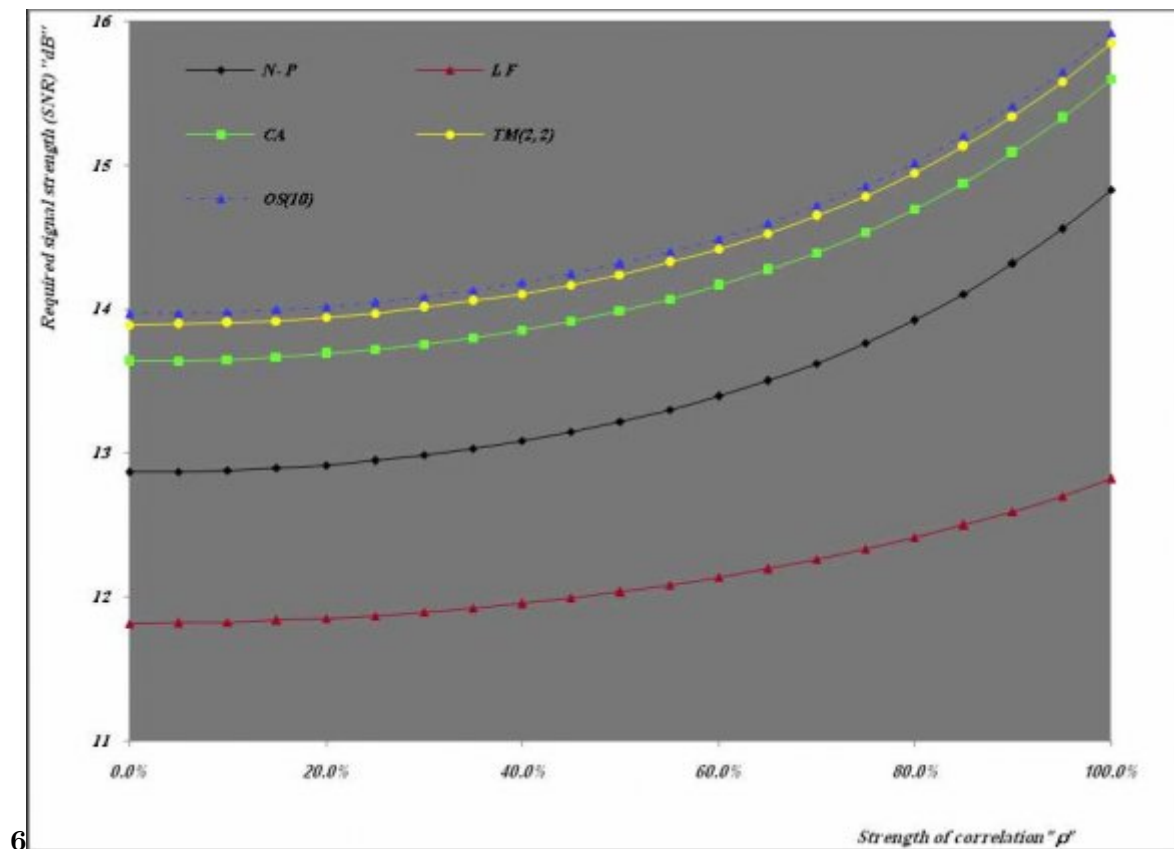
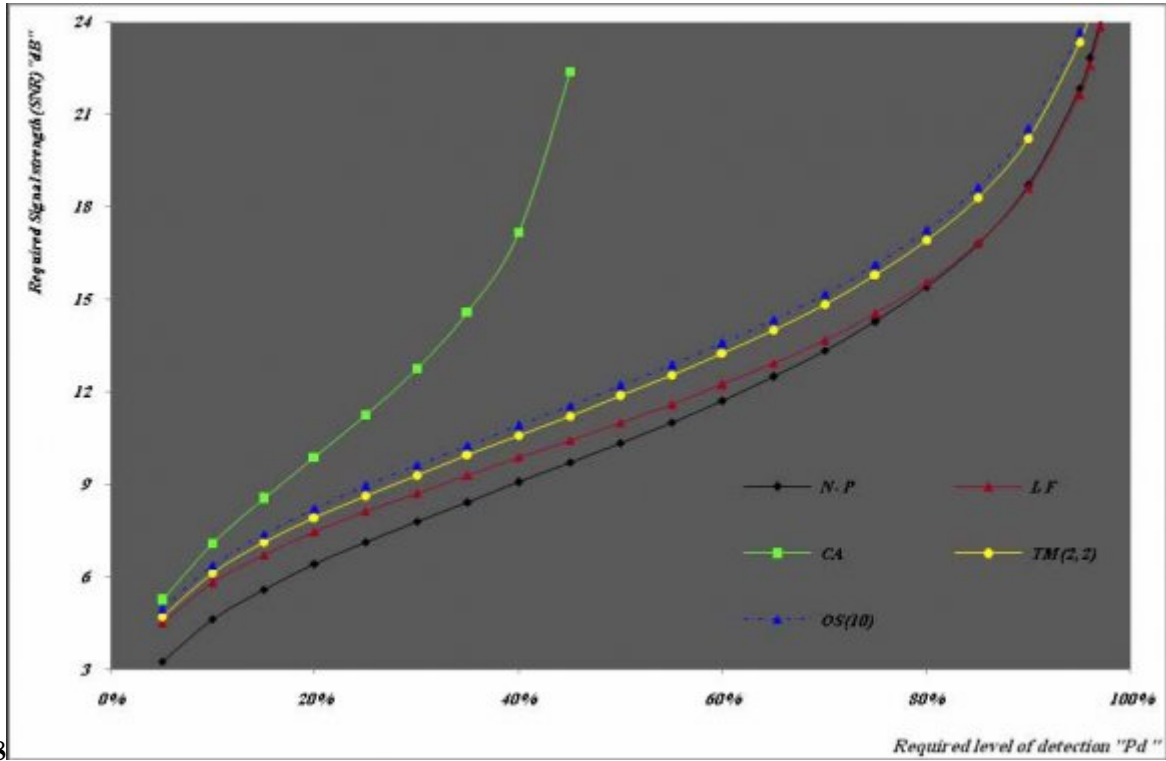
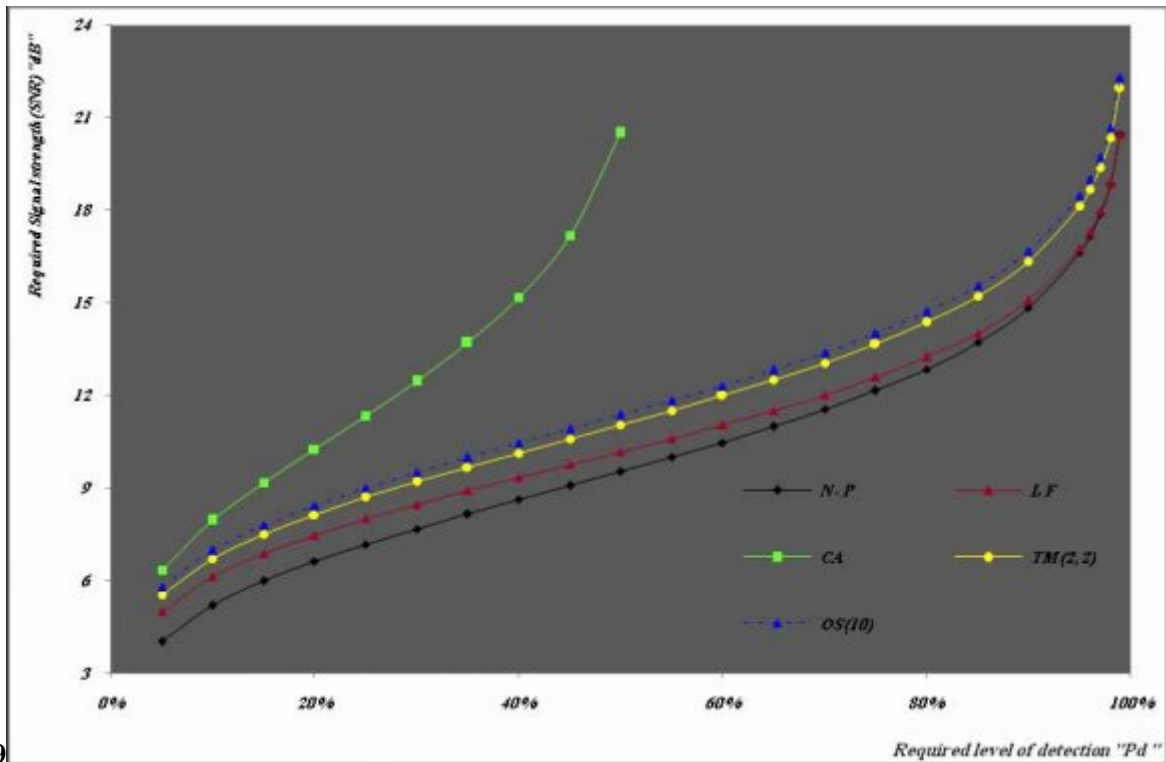


Figure 7: Fig. (6



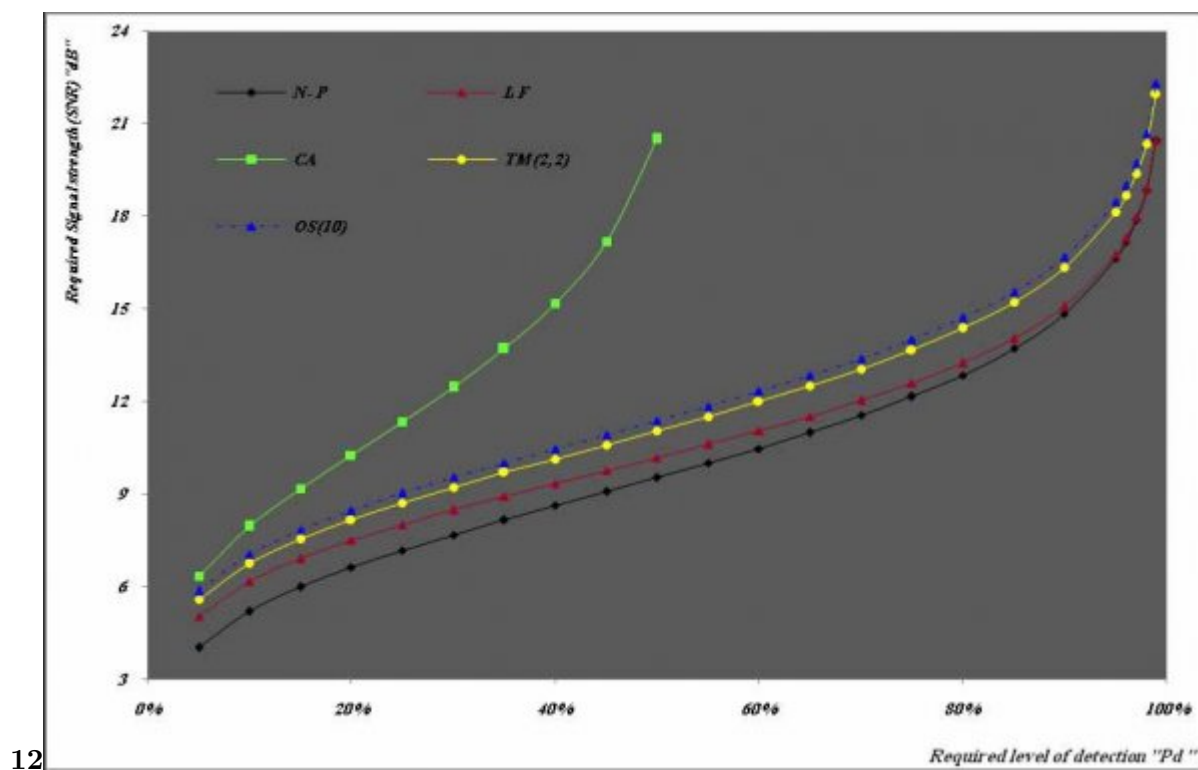
8

Figure 8: Fig. (8



9

Figure 9: Fig. (9



12

Figure 10: Fig. (12

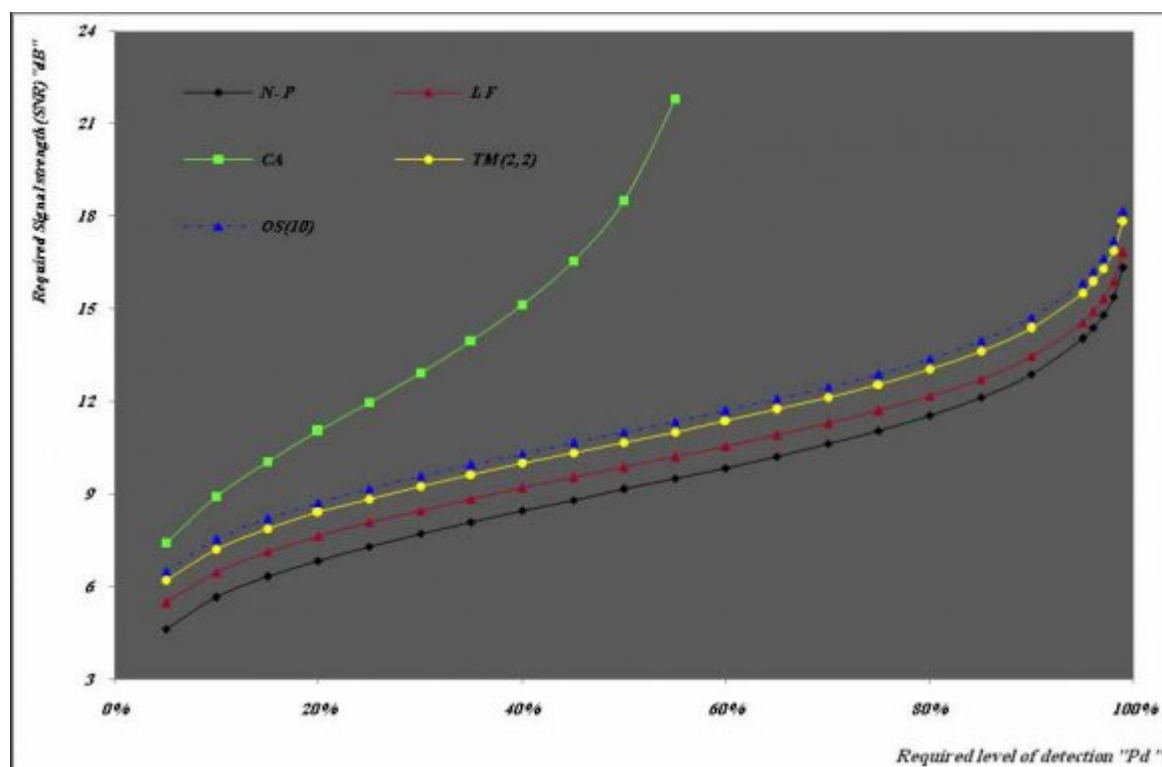


Figure 11:

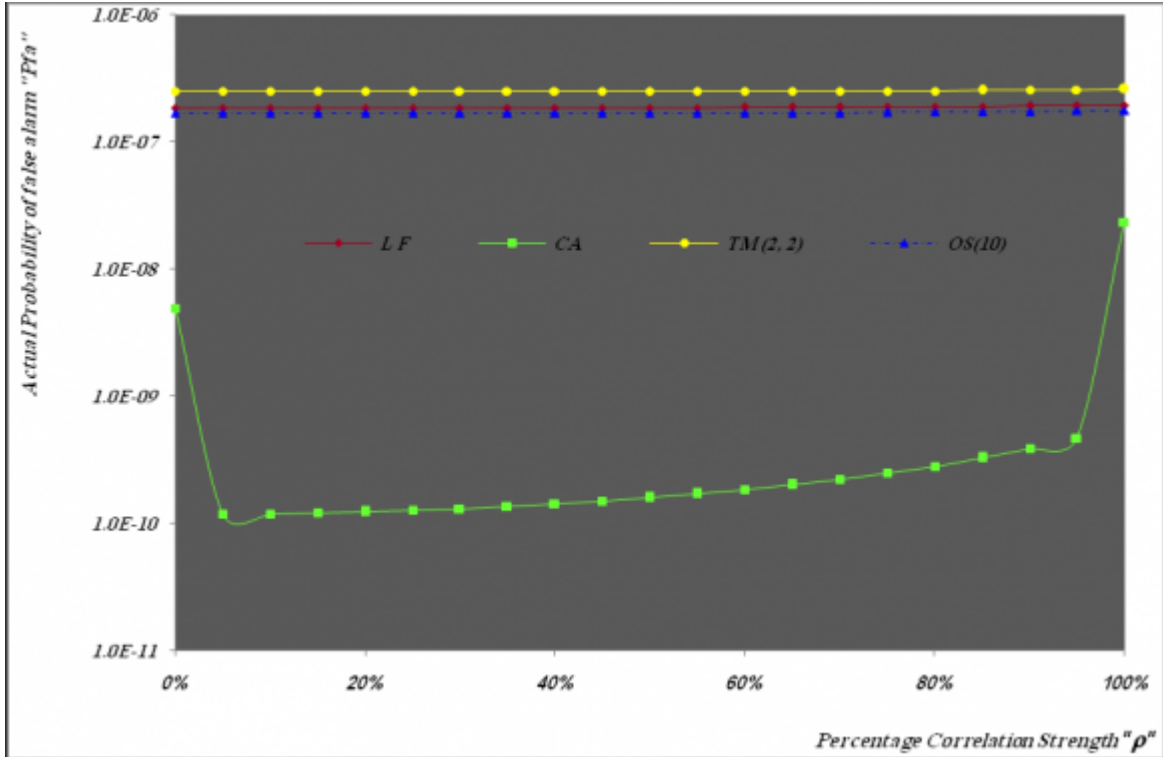


Figure 12:

1

CA Scenario FUSION RULE As Table I indicates, the appearance of ToI is OS Procedure TM Strategy demonstrated by the outcomes of rows 4, 6, 7, and 8.

Figure 13: Table 1 :

569 this research demonstrated. Thus, the LF strategy has the proficiency of choice en face of heterogeneous
570 situations.

571 [Anatolii et al. ()] ‘A New Class of Adaptive CFAR Methods for Nonhomogeneous Environments’. A Anatolii ,
572 Jin-Ha Kononov , Jin-Ki Kim , Gyoungju Kim , Kim . *Progress In Electromagnetics Research B* 2015. 64 p. .

573 [Zhao et al. (2001)] ‘A novel approach for CFAR processors design’. L Zhao , W Liu , X Wu , J S Fu . *Proc. of*
574 *the IEEE International Conference on Radar*, (of the IEEE International Conference on Radar Atlanta, GA)
575 1-3 May 2001. p. .

576 [Laroussi et al. (2007)] ‘A Performance Comparison of two time Diversity Systems using TM-CFAR Detection
577 for Partially Correlated Chi-Square Targets in Nonuniform Clutter and Multiple Target Situations’. Toufik
578 Laroussi , Mourad Barkat , Nassim Benadjina . *2007 IEEE International Conference on Signal Processing*
579 *and Communications (ICSPC 2007)*, (Dubai, United Arab Emirates) November 2007. p. .

580 [El Mashade ()] ‘Adaptive Detection Enhancement of Partially-Correlated χ^2 Targets in an Environment of
581 Saturated Interference’. M B El Mashade . *Recent Advances in Electrical & Electronic Engineering*, 2016.
582 9 p. .

583 [El Mashade (2006)] ‘Analysis of Cell-Averaging Based Detectors for χ^2 Fluctuating Targets in Multitarget
584 Environments’. M B El Mashade . *Journal of Electronics (China)* November 2006. 23 (6) p. .

585 [El Mashade ()] ‘Analytical Performance Evaluation of Optimum Detection of χ^2 Fluctuating Targets with
586 M-Integrated Pulses’. M B El Mashade . *Electrical and Electronic Engineering* 2011. 1 (2) p. .

587 [Farrouki and Barkat (2005)] ‘Automatic censoring CFAR detector based on ordered data variability for non-
588 homogeneous environments’. A Farrouki , M Barkat . *IEE Proc.-Radar Sonar Navig*, February 2005. 152 p.
589 .

590 [Md et al. ()] ‘Detection Capability and CFAR Loss Under Fluctuating Targets of Different Swerling Model for
591 Various Gamma Parameters in radar’. Md , Mohammed Islam , -E-Haider Hossam . *IJACSA) International*
592 *Journal of Advanced Computer Science and Applications* 2018. 9 (2) p. .

593 [Machado-Fernández et al. (2017)] *Evaluation of CFAR detectors performance*, J R Machado-Fernández , N
594 Mojena-Hernández , J Bacallao-Vidal . December 2017. 14 p. .

595 [Lopez-Estrada and Cumplido ()] ‘Fusion center with neural network for target detection in background clutter’.
596 Santos Lopez-Estrada , René Cumplido . *Proc. of the Sixth Mexican International Conference on Computer*
597 *Science (ENC’05)*, (of the Sixth Mexican International Conference on Computer Science (ENC’05)) 2005.

598 [Ivkovi ? et al. (2013)] ‘Fusion CFAR detector in receiver of the software defined radar’. D Ivkovi ? , B Zrni? ,
599 M Andri? . *Proc. of the International Radar Symposium IRS-2013*, (of the International Radar Symposium
600 IRS-2013 Dresden, Germany) June 2013. p. .

601 [El Mashade (2018)] ‘Heterogeneous Performance Analysis of the New Model of CFAR Detectors for Partially-
602 Correlated χ^2 -Targets’. M B El Mashade . *Journal of Systems Engineering and Electronics* February 2018.
603 29 (1) p. .

604 [El Mashade ()] ‘Inhomogeneous Analysis of Novel Model of CFAR Approaches to Detect Two-Degrees of
605 Freedom Partially-Correlated χ^2 -Targets’. M B El Mashade . *WSEAS Transactions on Communications*
606 2021. 20 p. .

607 [El Mashade ()] ‘Inhomogeneous Performance Evaluation of a New Methodology for Fluctuating Target Adaptive
608 Detection’. M B El Mashade . *Progress In Electromagnetics Research C* 2021. 107 p. .

609 [El Mashade ()] ‘M-Sweeps multi-target analysis of new category of adaptive schemes for detecting χ^2 -
610 fluctuating targets’. M B El Mashade . *Journal of Information and Telecommunication* 2020. 4 (3) p. .

611 [El Mashade (1996)] ‘Monopulse detection analysis of the trimmed mean CFAR processor in nonhomogeneous
612 situations’. M B El Mashade . *IEE Proc. Radar, Sonar Navig* April 1996. 143 (2) p. .

613 [El Mashade (1999)] ‘Partially correlated sweeps detection analysis of mean-level detector with and without
614 censoring in non ideal background conditions’. M B El Mashade . *Int. J. Electron. Commun. (AE?)* Feb.
615 1999. 53 (1) p. .

616 [El Mashade (2014)] ‘Partially-Correlated χ^2 Targets Detection Analysis of GTM-Adaptive Processor in the
617 Presence of Outliers’. M B El Mashade . *I.J. Image, Graphics and Signal Processing* Dec. 2014. 7 (12) p. .

618 [El Mashade ()] ‘Performance Analysis of OS Structure of CFAR Detectors in Fluctuating Target Environments’.
619 M B El Mashade . *Progress In Electro magnetics Research C* 2008. 2 p. .

620 [El Mashade ()] ‘Performance superiority of CA-TM model over N-P algorithm in detecting χ^2 fluctuating
621 targets with four-degrees of freedom’. M B El Mashade . *Int. J. Systems, Control and Communications* 2020.
622 11 (1) p. .

623 [Wang ()] *Radar Systems: Technology, Principals and Applications*, W Q Wang . 2013. Nova Science Publishers,
624 Inc.